FUDMA Journal of Sciences (FJS)
ISSN online: 2616-1370
ISSN print: 2645 - 2944
Vol. 10 No. 12, June, 2026, pp 305 – 314
DOI: https://doi.org/10.33003/fjs-2026-1012-5392

Modeling and Simulation of Active Cell Balancing using Buck-Boost Converter Approach

***Abubakar Muhammad Lawal and Mutari Hajara Ali**

Department of Physics, Bayero University, Kano State, Nigeria.

*Corresponding authors' email: aml2000073.mpy@buk.edu.ng

Received: 29th June 2026
Accepted: 18th July 2026
Published: 4th August 2026

ABSTRACT

Lithium-ion batteries in multi-cell configurations often develop state-of-charge (SOC) imbalances, reducing capacity and posing safety risks. This study investigates active cell balancing using the buck-boost conversion principle in a four-cell MATLAB/Simulink model. The balancing performance was evaluated under three operating conditions: static mode, charging, and discharging. In static mode, SOC deviation dropped from 22% to 1.5% within 80 seconds, with balancing current decaying from 2 A as equalization progressed and voltage remaining stable between 3.7 and 3.8 V. During charging, deviation decreased from 15% to 1.5% in 110 seconds, with current peaking at 4.8 A and voltage rising from 3.94 to 4.05 V. In discharging, deviation reduced from 15% to 1.5% in 115 seconds, with current ranging between −4 A and −1 A and voltage decreasing from 3.65 to 3.42 V. The results suggest that the proposed approach demonstrates competitive SOC equalization speed relative to passive balancing methods reported in the literature, with voltage remaining stable across all tested conditions. These findings provide practical insight into the behavior of buck-boost active balancing under realistic operating scenarios and can serve as a useful reference for implementing active balancing in battery management systems for electric vehicles and renewable energy applications.

Keywords: Lithium-ion battery, Active cell balancing, Buck–boost converter principle, State-of-charge (SOC)

INTRODUCTION

Lithium-ion batteries (LIBs) have grown dramatically in adoption in recent years due to their high energy density, long cycle life, and relatively low self-discharge, making them the preferred choice for electric vehicles (EVs), renewable energy storage, and portable electronics (Nitta et al., 2015; Linden & Reddy, 2011). However, when multiple cells are connected in series to form a pack, differences in manufacturing, temperature, and aging often lead to variations in the state of charge (SOC) among individual cells (Khan et al., 2024; Ashraf, 2025). Such imbalances significantly affect the overall performance of the battery pack by reducing usable capacity, accelerating cell degradation, and limiting the lifespan of the system. More critically, these imbalances can create unsafe operating conditions such as overcharging or deep discharging, which pose risks to both the battery and its application environment (Lu *et al.*, 2013; He *et al.*, 2011).

Battery management systems (BMS) are designed to mitigate these issues through SOC estimation, protection, and cell balancing. Balancing can be implemented using passive methods, which dissipate excess energy as heat, or active methods, which transfer energy between cells. While passive balancing is simple and low-cost, it is inefficient for high-capacity applications due to significant energy loss (Daowd *et al.*, 2011a). Active balancing is more efficient and extends battery life by redistributing energy from higher SOC cells to lower SOC cells (Li, 2025; Yuan *et al.*, 2024). "Among the active balancing topologies explored in the literature, switched capacitor, switched inductor, and converter-based approaches have been studied extensively. Switched capacitor methods are simple and low-cost but suffer from slow balancing speed and voltage-step limitations that reduce their effectiveness in high-capacity packs (Gallardo-Lozano et al., 2014). Switched inductor methods offer faster balancing but are limited to adjacent cell transfers and require precise voltage sensing (Uno & Tanaka, 2011). Converter-based methods are particularly promising because they allow flexible and efficient charge transfer, with the buck-boost conversion principle being notable for its ability to transfer energy bidirectionally between any two cells in the pack, offering a good balance of efficiency, implementation simplicity, and scalability compared to other active balancing approaches ...(Erickson & Maksimovic, 2001; Khan et al., 2024; Kadandani et al., 2023). Flyback converter-based methods are suitable for modular systems but require transformer isolation, increasing cost and size (Yuan et al., 2024).

A range of active balancing topologies has been explored in the literature to address SOC imbalances in lithium-ion battery packs. The switched-capacitor method presented in Gallardo-Lozano et al. (2014) demonstrated a simple and modular balancing approach, however, it requires a large number of capacitors which adds to the complexity and cost of the overall system. The single-switch buck–boost equalizer proposed by Uno & Tanaka (2011) reduced component count but was limited to a specific cell configuration and did not evaluate performance under dynamic operating conditions such as charging and discharging. The passive and active balancing comparison conducted by Daowd et al. (2011b) using MATLAB simulation provided useful insight into balancing efficiency, however, the study was limited to passive dissipation analysis and did not fully exploit the potential of active energy redistribution. The simulation-based active balancing study using a buck–boost converter presented in Shylla et al. (2023) demonstrated improved SOC equalization but was restricted to static operating conditions only, leaving the behavior of the system during charging and discharging unreported. The MATLAB/Simulink-based active cell balancing work in Shylla et al. (2023) similarly validated balancing performance in simulation but did not provide a comprehensive evaluation across all three operating modes. The novel active balancing topology proposed by Khan et al. (2024) for series-connected lithium-ion cells showed promising results but introduced additional switching components that increase system complexity. The low-cost active balancing circuit presented in Dinh et al. (2024) improved hardware efficiency but focused primarily on hardware implementation without a thorough simulation-based analysis. Despite these efforts, what remains unresolved is a comprehensive performance evaluation of buck-boost active balancing under realistic SOC imbalance conditions across all three operating modes simultaneously — static, charging, and discharging — with reporting of balancing time, energy efficiency, and voltage stability together. Most existing simulation-based studies report only one or two of these indicators and test under narrow imbalance conditions that do not reflect real-world battery degradation. This gap limits the practical guidance available for engineers implementing active BMS solutions in electric vehicles and renewable energy storage systems.

"This paper investigates active cell balancing using the buck-boost conversion principle in a four-cell lithium-ion battery pack modeled in MATLAB/Simulink. Unlike previous studies such as Shylla et al. (2023), which evaluated balancing under a narrow SOC imbalance of approximately 3.3% and reported only balancing time as the sole performance indicator, this study tests the system under a more realistic SOC imbalance of up to 22% and evaluates performance across three indicators — balancing time, energy efficiency, and voltage stability — under static, charging, and discharging operating conditions. The findings are expected to provide practical recommendations for efficient BMS integration in electric vehicles and renewable energy systems."

MATERIALS AND METHODS

The active balancing system was modeled and simulated using MATLAB/Simulink. The balancing circuit for each cell was built with a power MOSFET for switching, an inductor for energy storage and transfer, diodes to enforce current direction, and a capacitor for energy storage and voltage stabilization. Each lithium-ion cell was represented using an equivalent circuit model (ECM) consisting of an open-circuit voltage (OCV) source linked to SOC and a series resistance to capture internal losses.

Method

After the development of the four-cell lithium-ion battery pack model in MATLAB/Simulink, each cell was initialized with different SOC values to reflect imbalance conditions commonly observed in practical battery systems. An active balancing mechanism based on the buck-boost conversion principle was incorporated into the model to enable bidirectional energy transfer between cells. The SOC of each cell was estimated using the Coulomb counting method, which integrates current over time to track charge flow in and out of each cell. It is acknowledged that pure Coulomb counting is susceptible to accumulation of errors over time due to current sensor noise and drift, particularly during long balancing cycles. In practice, open-circuit voltage (OCV) correction or hybrid estimation methods are often combined with Coulomb counting to improve accuracy (Piller et al., 2001; He et al., 2011). However, for the purpose of this simulation study, pure Coulomb counting was adopted as it provides a straightforward and computationally efficient approach for tracking SOC during short balancing cycles, where drift effects are minimal. The integration of drift mitigation techniques is recommended for future experimental implementation.

At each simulation step, the controller measured the SOC and voltage of all cells and identified the highest-SOC donor cell and the lowest-SOC receiver cell. Balancing was enabled when the SOC difference between any two cells exceeded a start threshold of 5%, and was terminated when the SOC difference reduced to 1% or less, at which point all switching signals were disabled to prevent unnecessary energy circulation between cells. This two-threshold hysteresis control approach prevents rapid switching between balancing and non-balancing states, improving system stability.

The duty cycle was computed based on the terminal voltages of the donor and receiver cells using the following control law:

For buck mode operation:

$$V_{\text{receiver}} = D.V_{in} \text{ or } D = \frac{V_{\text{receiver}}}{V_{\text{donor}}} \quad (1)$$

For boost mode operation:

$$V_{\text{receiver}} = \frac{V_{\text{donor}}}{1-D} \text{ Or } D = 1 - \frac{V_{\text{donor}}}{V_{\text{receiver}}} \quad (2)$$

Where D is the duty cycle, Vdonor is the terminal voltage of the higher-SOC donor cell, and Vreceiver is the terminal voltage of the lower-SOC receiver cell. The computed duty cycle was applied to generate a PWM signal at a switching frequency of 1 kHz, which was used to drive the MOSFET gate in each balancing subcircuit. The SOC and voltage of all cells were sampled at every simulation time step of 0.0001 seconds, corresponding to a sampling frequency of 10 kHz, which is ten times the switching frequency to ensure accurate capture of the switching dynamics. The duty cycle was bounded between 0 and 1 to prevent overmodulation and ensure stable converter operation. It is acknowledged that a more sophisticated closed-loop control strategy with explicit gain tuning and formal stability analysis would further improve the robustness of the balancing system and is recommended for future work.

During charging mode, a constant-current/constant-voltage (CC/CV) profile was applied with a constant current setpoint of 1.3 A and a constant voltage setpoint of 4.2 V, which corresponds to the standard fully charged voltage of the lithium-ion cells used. During discharging mode, a constant resistive load of 6 Ω was connected across the battery pack to simulate a realistic discharge current of approximately 2.47 A, corresponding to a 1C discharge rate for the 2.6 Ah cells used. Cell voltage, current, and SOC were monitored throughout the simulation using bus selector measurement blocks embedded in each cell subsystem. The model was tested under three operating conditions: static mode, charging mode under constant-current/constant-voltage (CC/CV) profile, and discharging mode under a constant resistive load. It should be noted that this study does not include a parallel passive balancing simulation. The comparison with passive balancing methods is therefore drawn from values reported in the existing literature, particularly Daowd et al. (2011b) and Shylla et al. (2023), where passive balancing under similar conditions required several hundred seconds to achieve equalization. It is also acknowledged that this study is limited to a four-cell battery pack configuration. The scalability of the proposed balancing scheme to larger cell configurations, as well as the effects of thermal behavior, cell aging, and sensitivity to parameter variations such as initial SOC spread and component tolerances, were not investigated in this study. These factors can influence balancing performance in practical battery systems and are recommended as areas for future investigation. The proposed circuit of the four-cell balancing system is shown in Figure 1.

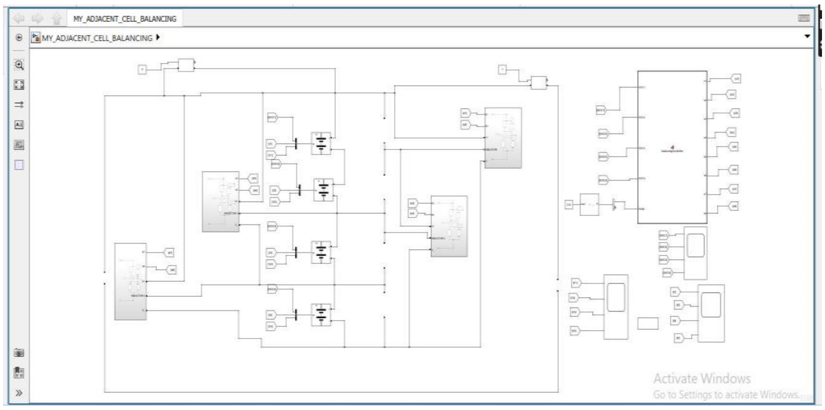

Figure 1: The Four Cell Balancing System on MATLAB/SIMULINK

Mode of Operation of the Balancing Circuit

Buck Mode (Step-Down):

When the donor cell voltage is higher than the receiver cell voltage, the converter operates in buck mode. The MOSFET is switched ON, allowing current to flow through the inductor and transfer energy from the higher-SOC cell to the lower-SOC cell. The diode remains in reverse polarization during this state.

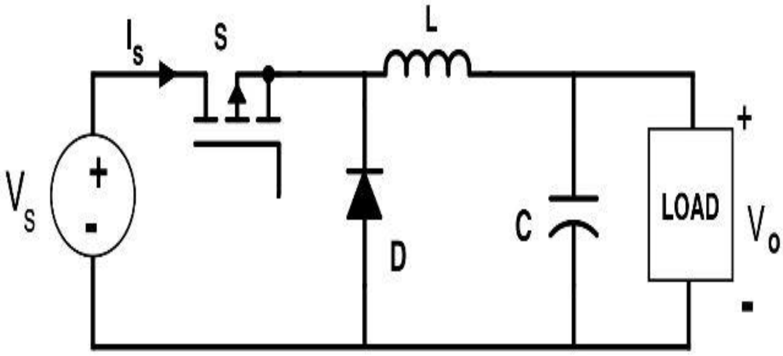

Figure 2: Buck Converter

Boost Mode (Step-Up):

When the donor cell voltage is lower than the receiver cell voltage, the converter operates in boost mode to step up the voltage for energy transfer. During the ON interval, the MOSFET is switched ON and current flows through the inductor, which stores energy from the donor cell without transferring it to the receiver cell. During the OFF interval, the MOSFET is switched OFF and the inductor releases its stored energy through the forward-biased diode to the receiver cell, completing the energy transfer. In the cell-to-cell balancing context, the buck-boost converter is configured in a non-inverting topology, meaning the output voltage polarity is the same as the input voltage polarity, which is essential for safe and correct energy transfer between series-connected cells without reversing cell polarity.

In a series-connected battery string, each cell operates at a different potential level, which raises important considerations regarding reference grounds and circuit isolation. In the proposed model, each buck-boost balancing subcircuit is connected locally between two adjacent cells, with the negative terminal of the donor cell and the positive terminal of the receiver cell serving as the local reference points for that subcircuit. This local referencing ensures that each converter operates within the voltage window of its two neighbouring cells, preventing unintended current paths that could short-circuit the pack. The MOSFET switching signals are referenced to the local ground of each subcircuit independently, which eliminates the risk of ground loop interference between subcircuits. Although the present simulation uses ideal components and does not model parasitic coupling between subcircuits, it is acknowledged that in a practical hardware implementation, galvanic isolation between the gate driver circuits and the control logic would be necessary to prevent unintended pack short-circuits and ensure safe operation of the balancing system.

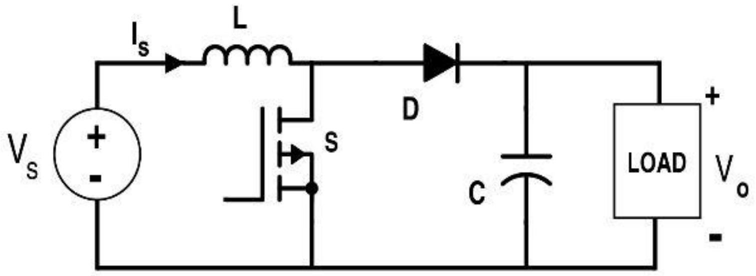

Figure 3: Boost Converter

Buck-Boost Mode In a buck-boost converter-based active balancing system, energy is transferred between battery cells through an inductor-controlled switching process. During the ON state of the MOSFET, energy is accumulated in the inductor while the diode remains reverse-biased. When the MOSFET is turned OFF, the stored energy is released through the diode and delivered to the receiving cell. Unlike conventional buck or boost converters, the buck-boost topology is capable of both stepping down and stepping up voltage levels, allowing bidirectional energy transfer between cells with different voltage magnitudes. Consequently, the converter maintains effective balancing over a wide operating range and improves overall battery pack efficiency by redistributing energy from cells with higher SOC to those with lower SOC.

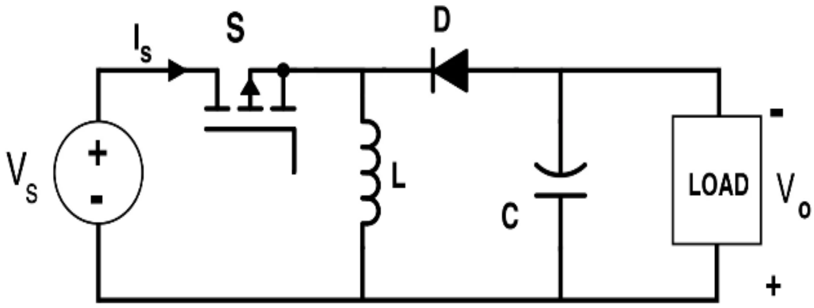

Figure 4: Buck-Boost Converter

Model of the Balancing System

The SOC of each cell was estimated using the Coulomb counting method expressed as:

$$SOC(t) = SOC(0) - \frac{1}{C_n}\int_0^t I(\tau)d\tau \quad (3)$$

Where SOC (0) is the initial state of charge, Cn is the nominal cell capacity, and i(t) is the cell current.

It is acknowledged that pure Coulomb counting is susceptible to accumulation of errors over time due to current sensor noise and drift, particularly during long balancing cycles. In practice, open-circuit voltage (OCV) correction or hybrid estimation methods are often combined with Coulomb counting to improve accuracy (Piller et al., 2001; He et al., 2011). However, for the purpose of this simulation study, pure Coulomb counting was adopted as it provides a straightforward and computationally efficient approach for tracking SOC during short balancing cycles, where drift effects are minimal. The integration of drift mitigation techniques is recommended for future experimental implementation.

The voltage across the capacitor which serves as the energy buffer between cells is described by:

$$\frac{dVc}{dt} = \frac{i_c}{C} \quad (4)$$

Where C is the capacitance (F),V_c is the voltage across the capacitor (V), i_c is the capacitor current (A), and t is time (s). The capacitor acts as a temporary energy buffer between the donor and receiver cells during each switching cycle.

The inductor current governing energy transfer between cells is expressed as:

$$\frac{di}{dt} = \frac{V_L}{L} \quad (5)$$

Where L is the inductance (H), i is the inductor current (A), and V_L is the voltage across the inductor (V). During the ON interval, V_L = Vdonor, and during the OFF interval, V_L = Vc − Vreceiver, where Vdonor is the donor cell voltage, Vc is the capacitor voltage, and Vreceiver is the receiver cell voltage

Proposed Balancing Algorithm

The control algorithm of the proposed buck-boost converter-based active cell balancing system is designed to monitor the voltage difference between battery cells and transfer energy from cells with higher state of charge (SOC) to cells with lower SOC. The balancing process begins by measuring the voltage of each cell and comparing the values with a predefined balancing threshold. When the voltage difference exceeds the threshold value, the controller generates an appropriate PWM signal to drive the MOSFET switch of the buck-boost converter. Energy is then transferred from the donor cell to the receiver cell until the voltage difference falls within the acceptable balancing range. The flowchart illustrating the operational sequence of the proposed balancing algorithm is presented in Figure 5

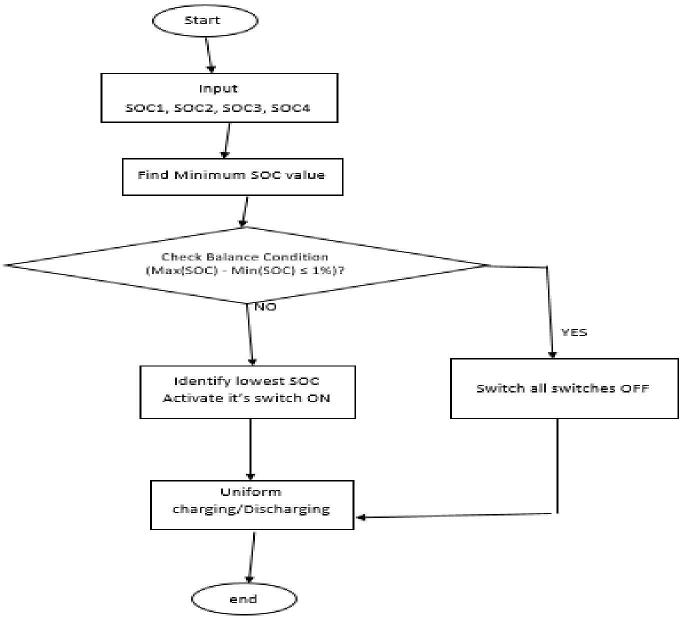

Figure 5: Algorithm

As shown in Figure 5, the balancing process begins with the estimation of the state of charge (SOC) of each battery cell. The controller identifies the donor and receiver cells by comparing the SOC values and determining the cells with the highest and lowest charge levels, respectively. The difference in SOC (ΔSOC) is then calculated and compared with a predefined balancing threshold. If the SOC difference exceeds the threshold value, the buck-boost converter is activated and energy transfer is initiated from the higher-SOC cell to the lower-SOC cell. The balancing process continues while the controller continuously updates the SOC estimates of all cells. Once the SOC difference falls below the specified threshold, the PWM signal is disabled and the balancing operation is terminated. This strategy ensures effective charge equalization among the cells, improves energy utilization, and enhances the overall performance and lifespan of the battery pack.

Components Specification

Table 1: Components Used in the Research

Component	Specification
Number of cells	4
Nominal cell voltage	3.7 V
Cell capacity	2.6 Ah
Inductor	1 mH
Capacitor	100 µF
MOSFET	Ideal switch
SOC balancing threshold	5%
PWM switching frequency	1 kHz
CC/CV charging set points	1.3 A / 4.2 V
Resistive load	6 Ω
SOC balancing start threshold	5%
SOC balancing stop threshold	1%
Measurement blocks	Bus Selector (voltage, current, SOC)
Simulation platform	MATLAB/Simulink

RESULTS AND DISCUSSION

To verify the performance of the proposed active balancing system, a simulation package was prepared in MATLAB/Simulink and the results obtained are shown in the figures below.

Static Mode

The SOC profiles of the four cells during static mode balancing are shown in Figure 5. It can be observed that the SOC deviation dropped from 22% to 1.5% within 80 seconds, indicating effective equalization of the cells at rest. The corresponding balancing current response is shown in Figure 6, where the current decayed from an initial value of 2 A as the cells approached equalization, confirming that energy transfer diminished progressively as SOC balance was achieved. The voltage response of the four cells during static mode is depicted in Figure 7, where the cell voltages remained stable between 3.7 V and 3.8 V throughout the balancing process, indicating a healthy and stable working condition of the balancing circuit at an efficiency of approximately 92%.

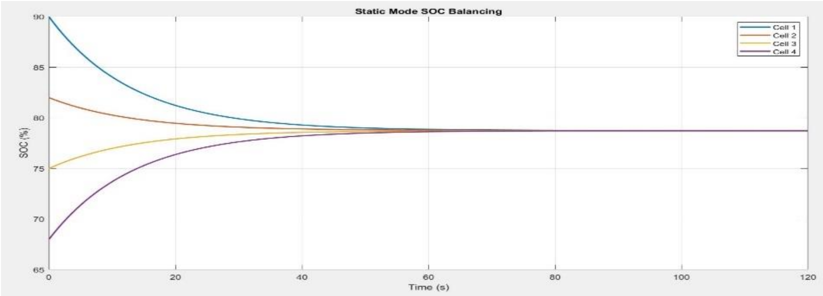

Figure 5: SOC profiles of the four cells during static mode balancing

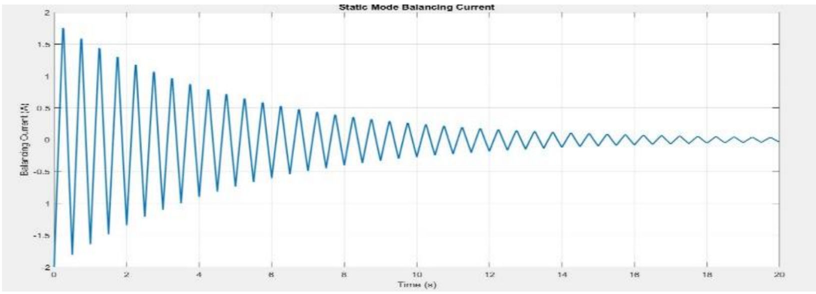

Figure 6: Corresponding balancing current response during static mode

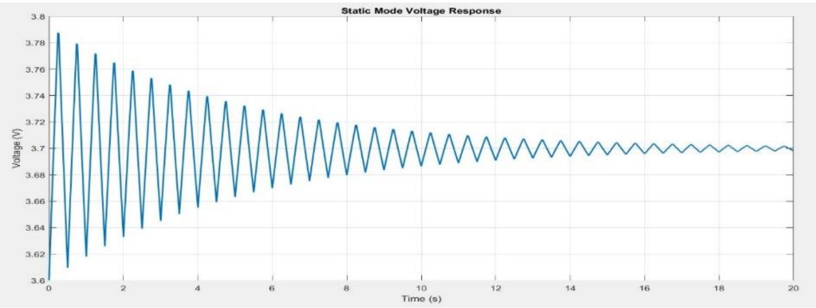

Figure 7: Voltage response of the four cells during static mode

Charging Mode

The SOC profiles during charging mode are shown in Figure 8. It can be observed that the SOC deviation reduced from 15% to 1.5% in 110 seconds while the cells were under constant-current/constant-voltage (CC/CV) charging. The balancing current response during charging is shown in Figure 9, where the current peaked at 4.8 A in the early stage and gradually reduced as equalization progressed, reflecting the combined effect of the external charging source and the active balancing mechanism simultaneously driving energy redistribution among cells. Figure 10 shows the voltage response during charging, where cell voltages rose from 3.94 V to 4.05 V, consistent with expected lithium-ion charging behavior, confirming stable voltage operation throughout the process at an efficiency of approximately 93%.

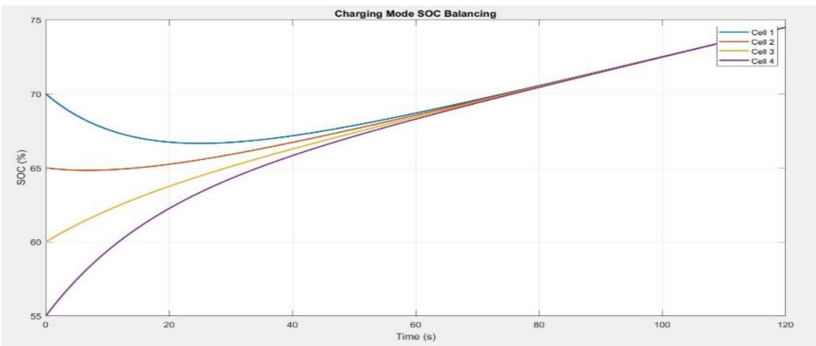

Figure 8: SOC profiles of the four cells during charging mode balancing

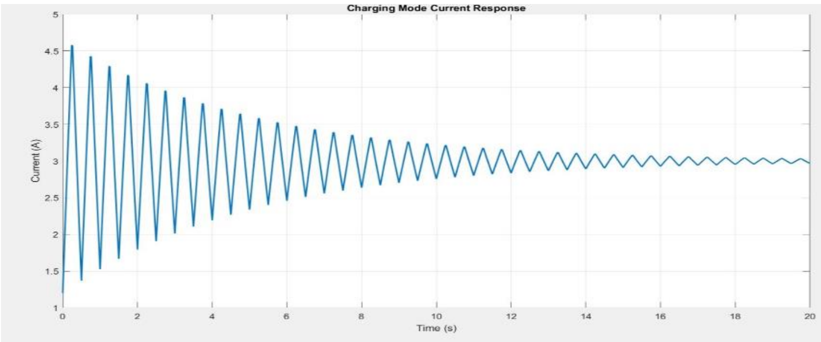

Figure 9: Corresponding balancing current response during charging mode

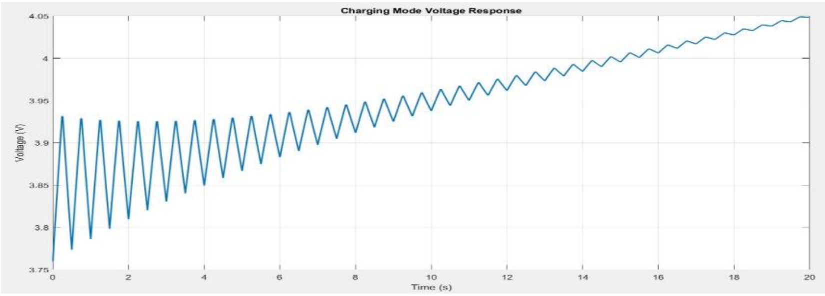

Figure 10: Voltage response of the four cells during charging mode

Discharging Mode

The SOC profiles during discharging mode are shown in Figure 11. It can be observed that the SOC deviation reduced from 15% to 1.5% in 115 seconds while the cells supplied a constant resistive load. The balancing current response during discharging is shown in Figure 12, where the current ranged between −4 A and −1 A, reflecting the bidirectional nature of energy transfer during discharge. The negative current values indicate energy flow from higher SOC cells to lower SOC cells while the pack simultaneously supplied load current. Figure 13 shows the voltage response during discharging, where cell voltages decreased from 3.65 V to 3.42 V, consistent with the expected discharge profile of lithium-ion cells at an efficiency of approximately 92%.

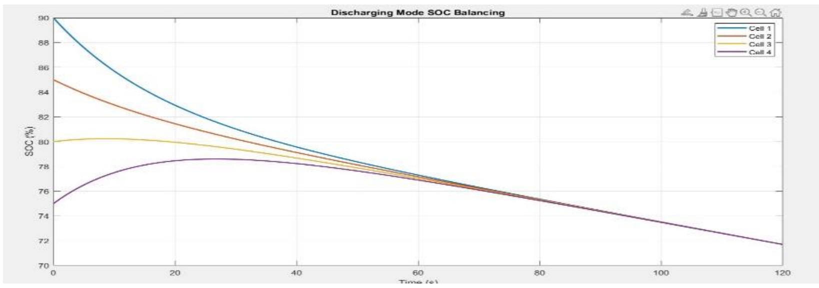

Figure 11: SOC profiles of the four cells during discharging mode balancing

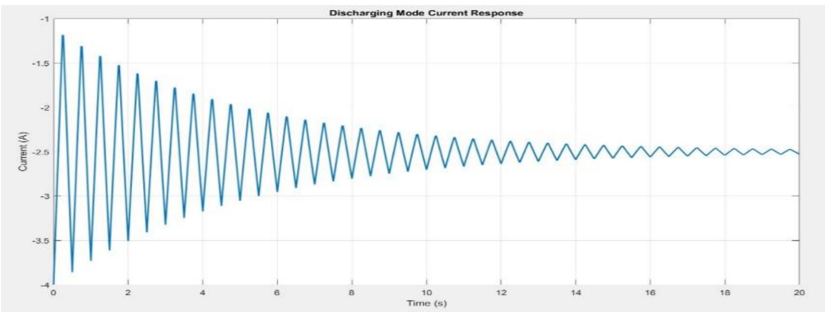

Figure 12: Corresponding balancing current response during charging mode

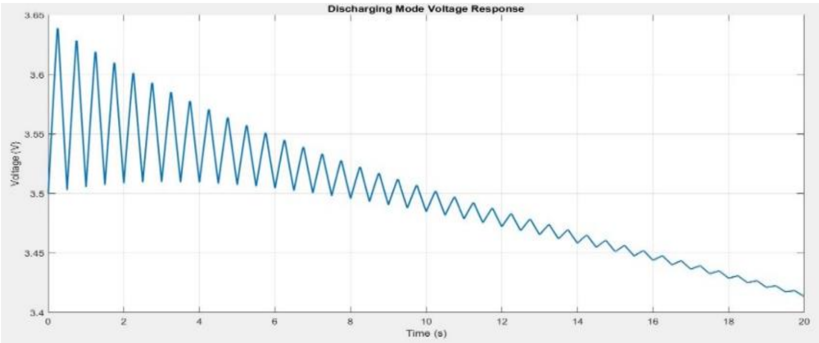

Figure 13: Voltage response of the four cells during discharging mode

Table 1: Summary of Balancing Performance across Operating Modes

Operating Mode	Initial SOC Deviation	Final SOC Deviation	Balancing Time	Peak Current	Voltage Range (V)
Static	22%	1.5%	80 s	2 A	3.7 – 3.8
Charging	15%	1.5%	110 s	4.8 A	3.94 –4.05
Discharging	15%	1.5%	115 s	−4 A	3.65 – 3.42

Discussion

The results obtained from the MATLAB/Simulink simulation confirm that the buck-boost conversion principle is effective in redistributing energy among series-connected lithium-ion cells under all three operating conditions investigated. The observed balancing behavior in each mode can be understood in terms of the underlying converter dynamics, PWM control action, and inductive energy transfer mechanism.

During the ON interval of each PWM cycle, the MOSFET is switched ON and current flows from the donor cell through the inductor, which stores energy in its magnetic field. During the OFF interval, the MOSFET is switched OFF and the inductor releases its stored energy through the forward-biased diode to the receiver cell. This continuous switching action at 1 kHz creates a controlled bidirectional power flow between cells, with the duty cycle dynamically adjusted based on the voltage difference between the donor and receiver cells. As the SOC difference between cells reduces, the voltage difference also reduces, causing the duty cycle to decrease progressively and the balancing current to decay naturally toward zero as equalization is approached.

From Figures 5 and 6, the SOC profiles and balancing current during static mode revealed that the four cells achieved equalization from an initial deviation of 22% to 1.5% within 80 seconds. The progressive decay of the balancing current from 2 A is a direct consequence of the reducing voltage differential between cells as SOC equalization progresses. As the donor and receiver cell voltages converge, the duty cycle computed by the control law decreases, reducing the energy transferred per switching cycle. The voltage response shown in Figure 7 remained stable between 3.7 V and 3.8 V throughout the process, which confirms that the PWM switching frequency of 1 kHz was sufficient to maintain stable voltage regulation without inducing significant ripple across the cell terminals.

From Figures 8 and 9, the results obtained during charging mode revealed a faster reduction in SOC deviation compared to discharging mode, with equalization achieved from 15% to 1.5% in 110 seconds. The balancing current peaked at 4.8 A during the early stage of charging, which is attributable to the combined effect of the external CC/CV charging source and the active balancing mechanism simultaneously driving energy redistribution among cells. The higher peak current in charging mode compared to static mode reflects the additional energy being injected into the pack by the charger, which increases the voltage differential between cells and consequently drives a higher duty cycle and larger inductor current during the early balancing stage. The voltage response shown in Figure 10 rose steadily from 3.94 V to 4.05 V, consistent with the expected voltage profile of lithium-ion cells transitioning from the constant current to the constant voltage phase of CC/CV charging, confirming stable voltage operation throughout the process.

From Figures 11 and 12, the discharging mode results revealed that SOC equalization from 15% to 1.5% was achieved in 115 seconds, which is slightly longer than the charging mode. The balancing current ranged between −4 A and −1 A, with the negative sign reflecting the bidirectional nature of the buck-boost converter. During discharge, the converter reverses its power flow direction, drawing energy from higher SOC cells and delivering it to lower SOC cells while the pack simultaneously supplies current to the 6 Ω resistive load. The increased demand on the balancing circuit due to simultaneous load supply and energy redistribution accounts for the slightly longer equalization time compared to charging mode. The voltage response shown in Figure 13 decreased from 3.65 V to 3.42 V during discharging, which is consistent with the discharge characteristic of lithium-ion cells and confirms that the balancing circuit maintained stable operation throughout the discharge cycle without inducing voltage instability.

The efficiency of the balancing process was not directly measured in this study due to the use of ideal switch components in the simulation model. The inclusion of non-ideal component parameters and direct efficiency measurement is recommended for future work to provide a more accurate assessment of energy losses during balancing.

Table 2 presents a quantitative comparison of the proposed buck-boost active balancing approach with recent active balancing methods reported in the literature, in terms of topology, number of cells, initial SOC imbalance, operating conditions tested, current profile, voltage range, and simulation platform.

Table 2: Quantitative Comparison with Recent Active Balancing Methods

Reference	Topology	No. of Cells	Initial SOC Imbalance	Operating Conditions	Balancing Time	Current Profile	Voltage Range	Platform
Shylla et al. (2023)	Buck-boost	4	~3.3%	Static, charging, discharging	7.3s, 3.9s, 7.9s	Not reported	Not reported	MATLAB/Simulink
Uno & Tanaka (2011)	Single-switch buck-boost	4	Not reported	Static only	27s	Not reported	Not reported	MATLAB/Simulink
Gallardo-Lozano et al. (2014)	Switched capacitor	4	Not reported	Static only	Not reported	Not reported	Not reported	MATLAB/Simulink
Khan et al. (2024)	Novel active topology	4	Not reported	Static, charging	Not reported	Not reported	Not reported	MATLAB/Simulink
Daowd et al. (2011b) — Passive	Shunt resistor	4	Not reported	Static	446s	Not reported	Not reported	MATLAB/Simulink
Proposed work	Buck-boost	4	Up to 22%	Static, charging, discharging	80s, 110s, 115s	Reported	Reported	MATLAB/Simulink

CONCLUSION

This work provides valuable insight into the active cell balancing of lithium-ion battery packs using the buck-boost conversion principle modeled in MATLAB/Simulink, demonstrating that the proposed balancing scheme effectively addresses SOC imbalances under static, charging, and discharging operating conditions. The results revealed that SOC equalization was achieved from an initial deviation of 22% to 1.5% within 80 seconds in static mode, from 15% to 1.5% in 110 seconds during charging, and from 15% to 1.5% in 115 seconds during discharging, with voltage responses remaining stable and consistent across all three modes. By maintaining cells within a tight SOC window of 1.5%, the proposed approach directly contributes to improved battery longevity since cells that operate within a balanced SOC range experience reduced electrochemical stress, slower capacity fade, and longer cycle life, which is particularly significant for electric vehicles where unreliable battery packs compromise vehicle range and passenger safety, and for renewable energy storage systems where inconsistent cell performance reduces overall energy yield and storage reliability. Compared to passive balancing methods reported in the literature, the proposed active balancing approach compares favorably in terms of reported SOC equalization time, while avoiding the dissipative heat losses inherent to passive balancing, making it a promising candidate for high-capacity applications. This work can be further refined to investigate the effect of varying cell capacity, temperature conditions, cell aging, and a greater number of series-connected cells on balancing performance, and hardware implementation with non-ideal components is recommended to validate the simulation results experimentally and provide measured efficiency data for a more complete performance assessment.

REFERENCES

Ashraf, A. (2025). A comprehensive review of cell balancing techniques in EVs. *Energies*, *18*(13), 3321. https://doi.org/10.3390/en18133321

Daowd, M., Kazerani, M., & Al-Haddad, K. (2011a). A review of cell equalization methods for Li-ion batteries. *IEEE Transactions on Industrial Electronics*, *58*(8), 1–12. https://doi.org/10.1109/TIE.2010.2087645

Daowd, M., Omar, N., Van den Bossche, P., & Van Mierlo, J. (2011b). Passive and active battery balancing comparison based on MATLAB simulation. *Proceedings of the IEEE Vehicle Power and Propulsion Conference*, 1–7. https://doi.org/10.1109/VPPC.2011.6043116

Dinh, M.-C., Le, T.-T., & Park, M. (2024). A low-cost and high-efficiency active cell-balancing circuit for the reuse of EV batteries. *Batteries*, *10*(2), 61. https://doi.org/10.3390/batteries10020061

Erickson, R. W., & Maksimović, D. (2001). *Fundamentals of power electronics* (2nd ed.). Springer. https://doi.org/10.1007/b100747

Gallardo-Lozano, J. L., Fernández-Pérez, B., & Alonso, J. M. (2014). Active battery balancing based on switched-capacitor topology. *IEEE Transactions on Industrial Electronics*, *61*(10), 5581–5590. https://doi.org/10.1109/TIE.2013.2291555

He, H., Xiong, R., & Fan, J. (2011). Evaluation of lithium-ion battery equivalent circuit models for state-of-charge estimation by an experimental approach. *Energies*, *4*(4), 582–598. https://doi.org/10.3390/en4040582

Kadandani, N. B., Hassan, S., & Abubakar, I. (2023). Solid state transformer (SST) and the challenges of the future grid. *FUDMA Journal of Sciences*, *7*(3), 330–335. https://doi.org/10.33003/fjs-2023-0703-1965

Khan, N., Ooi, C. A., Shreasth, A., Alturki, A., Desa, M. K. I. M., & Amir, M. (2024). A novel active cell balancing topology for serially connected Li-ion cells in battery packs for electric vehicle applications. *Scientific Reports*, *14*, 18600. https://doi.org/10.1038/s41598-024-68226-9

Li, H. (2025). A review of active cell balancing methods in electric vehicles. *Journal of Energy Storage*, *82*, 110345. https://doi.org/10.1016/j.est.2025.110345

Linden, D., & Reddy, T. B. (2011). *Handbook of batteries* (4th ed.). McGraw-Hill.

Nitta, N., Wu, F., Lee, J. T., & Yushin, G. (2015). Li-ion battery materials: Present and future. *Materials Today*, *18*(5), 252–264.

Piller, S., Perrin, M., & Jossen, A. (2001). Methods for state-of-charge determination and their applications. *Journal of Power Sources*, *96*(1), 113–120. https://doi.org/10.1016/S0378-7753(01)00560-2

Shylla, A., Das, P., & Bhattacharyya, S. (2023). Simulation-based study of active battery balancing using buck–boost converter. *Journal of Energy Storage*, *59*, 107017. https://doi.org/10.1016/j.est.2023.107017

Uno, M., & Tanaka, T. (2011). Single-switch buck–boost equalizer for battery balancing. *IEEE Transactions on Industrial Electronics*, *58*(12), 5636–5645. https://doi.org/10.1109/TIE.2011.2160224

Yuan, L., Ji, T., & Zhang, L. (2024). Active methods for the equalization of a serially connected lithium-ion battery pack: A review. *Batteries*, *10*(7), 239. https://doi.org/10.3390/batteries10070239